1-1-2003

Evidence for trap conversion instability in hydrogenated amorphous silicon

Puneet Sharma
Iowa State University

Evidence for Trap conversion instability in hydrogenated Amorphous Silicon

by

Puneet Sharma

A thesis submitted to the graduate faculty

in partial fulfillment of the requirements for the degree of

MASTER OF SCIENCE

Major: Electrical Engineering

Program of Study Committee:
Vikram L. Dalal, Major Professor
Gary Tuttle
Rana Biswas

Iowa State University

Ames, Iowa

2003

Graduate College
Iowa State University

This is to certify that the master's thesis of

Puneet Sharma

has met the thesis requirements of Iowa State University

Signatures have been redacted for privacy

TABLE OF CONTENTS

LIST OF FIGURES

LIST OF TABLES

ABSTRACT

The hydrogenated amorphous silicon (a-Si:H) has been widely studied and used semiconductor. With all the excellent optical and electrical properties that it provides, there have been few characteristics which are not exactly understood till now that has hampered its extensive commercial use. Understanding the stability of these materials has been one of the major challenges being faced leading to extensive studies in past 25 years. It has been postulated that there are two different states in the sub-band gap of a-Si:H playing a dominant role. One state that has been proved and studied a lot is that of neutral dangling bonds and the other state being the charged dangling bonds. It has been known for some time that there are two distinct types of recovery during annealing of amorphous silicon after degradation during light soaking. While the previous studies of electron $\mu\tau$ (mobility lifetime) product Vs α (alpha) have been able to find these defects during the annealing, the plot is a straight line during degradation.

The research studies the role of these charged defects in the degradation process and study for its kinetics during the exposure stage which has not been seen before. The results obtained from the stability experiments (exposure to xenon and subsequent annealing at different times) of oxygen doped films made in ECR-PECVD system have shown the conversion of negatively charged negatively correlated states into neutral dangling bonds with the capture of charge carriers; at a different energy location. These increased neutral dangling bonds explain for the decrease in photoconductivity. A quantitative model has been developed explaining the above kinetics and also supporting Adler's trap to dangling bond conversion model as shown by the changes in shape of the sub-gap absorption curve would change during the degradation, with a decrease in the region where the D^- bonds exist, and an increase in the region where D^0 exist. Most of the studies done at a particular energy failed to see the increase of these states which were at a different location in the gap and were clearly seen in α Vs E plots. The presence of these charged defects have been traced back to accidental O doping.

CHAPTER 1

INTRODUCTION

Amorphous Silicon as a Photovoltaic Material:

Hydrogenated amorphous silicon is a very widely used semiconductor and has applications in fields requiring large area microelectronics, such as active matrix flat panel display, light emitting diodes, thin film transistors and multi-junction solar cells.

The electrical and optical properties of hydrogenated amorphous silicon have made it a very interesting and an extensively used photovoltaic material. In comparison to crystalline silicon (c-Si), in a-Si their inherent disorder by relaxing the momentum conservation rule, leads to a high optical absorption for a 200–500 nm thick film. Other than abundant raw-material, the low temperature requirement facilitates the use of low cost substrate materials such as float glass, metal or plastic foils. All these lead to a short energy pay back time and substantial cost reduction potential compared to conventional crystalline silicon technology. The low material cost and proven manufacturability of a-Si: H solar modules make them ideally suited for low-cost terrestrial applications and thin film transistor's..

Several key features that make a-Si: H an attractive photovoltaic material is:

- Being a direct band gap material it has a very high absorption coefficient ($>10^5$ cm^{-1}) over the majority of the visible spectrum, making extremely thin film (700-2000 Å) possible.
- The optical band gap ~ 1.7 eV is optimum for obtaining high conversion efficiencies.
- The raw materials silicon and hydrogen are both abundant materials.
- A simple low temperature deposition process can be used to make large area and uniform films and devices

- The material can be easily doped n and p type using boron, phosphorus etc respectively.
- Large scale integration of different cells is simple and easily accomplished.

Motivation behind the Research:

Nowadays world record efficiencies demonstrate stable active-area conversion efficiencies in excess of 13%, although the theoretical estimates indicate that a stable efficiency of 16% is achievable with rather elegant improvement in the performance of the component cells of the triple-junction a-Si structure [18]. The total-area efficiency of a solar cell module is usually 5–7% lower. Several factors contribute to this difference: most importantly, the active area efficiency does not include the shadow loss due to the grids, which is typically 4–6%, besides the modules are encapsulated to provide protection against the environment, and this causes an additional loss. As a consequence of the fundamental goals for photovoltaic systems (i.e. higher P_{max}), research and fabrication in this area has shifted towards the large area modules; instead of the simple cells.

Now this is where the amorphous semiconductors become so attractive- the ease with which they can be deposited for large area modules. This is because the amorphous silicon is a solid state material made out of silicon atoms which are arranged in a lattice lacking long range order. Locally, the electronic bonds between the neighboring elements in the amorphous network are almost identical to their crystalline counterparts. Small distortions, however, destroy any long range periodicity.

All the above features make hydrogenated amorphous silicon – a material that has generated vast interests in scientific community and its complete understanding is primary objective of many of research groups all around the world. It has been seen that in these modules, light degradation plays a key rule in decreasing the total achievable efficiency, and in all these approaches either from material science or engineering point of view an accurate understanding of the degradation mechanisms is the main focus. The stability of amorphous silicon has been a major hindrance in the path of it to rule the semiconductor company. This

challenging problem has been extensively studied for last 25 years but still there in no complete and accurate explanation of the problem and its solution.

Overview of the Problem:

Stability is one of the major issues hampering amorphous silicon being commercially used as photovoltaic material for large scale power applications. In 1977 D. Staebler and C. Wronski [1] discovered that the electronic quality of hydrogenated amorphous silicon degrades under illumination. Even at the moderate light intensities like 1 sun, the photo and dark conductivities decrease with illumination [Staebler and Wronski] and since then this effect is defined as Staebler Wronski effect (SWE). The observed changes were found to be reversible by annealing of the a-Si: H samples above (>150 ^{0}C). The deleterious influence of this SWE can be mitigated by various techniques, but so far it has not been possible to eliminate the SWE or even fully understand it. Lot of research has been done all over the world to comprehend it or suppress it, but not complete success has been obtained till date.

First step was the discovery that light induced degradation in photo and dark conductivity is accompanied by an increase in the electron spin resonance signature of the unsaturated three-fold coordinated silicon bonds called 'dangling bonds' (DB's) [2,3]. If the material is directly evaporated on the glass slide, it contains around 10^{19} to 10^{21} cm^{-3} of these DB defects which makes the material dead. But the introduction of hydrogen from 2-15%, decrease these defects by several orders of magnitude. Such hydrogenated amorphous silicon is good photoconductive material for solar cells, thin film transistors and flat panel display applications. The discovery of the increase in DB density with illumination pointed to the cause of SWE, because the DB's have states at mid-gap which acts as efficient recombination centers for photo-generated charged carriers, such that the life time of the photo-induced carriers decrease with increasing DB density. They also lead to shift of the Fermi-Level E_f towards the mid-gap. Direct evidence for the creation of states in the mobility gap of a-Si:H by prolonged illumination comes from various experiments: reversible changes in the field effect [4,5], the deep level transient spectroscopy response [6] defect luminescence [7], sub-band gap measurement [8], and increase of Si dangling bonds in

Electron Spin resonance measurement [2,3]. The qualitative conclusions for most of the authors agree but the quantitative conclusions from the different experiments, however, do not agree at all. Discrepancies exits about the absolute density of these defects, their position in the mobility gap and whether one or more types of defects can be created by illumination.

There has been lot of studies that neutral dangling bonds are the responsible for the degradation. Also the theories that charged dangling bonds exist and have considerable effect on the kinetics of degradation have been evolved. H motion has been strongly linked to the annealing of the light induced defects [9]. Meta-stability is also observed down to temperatures as low as 4 K [10] where the long range motion is presumably absent. A power law dependence of $t^{0.3}$ is also observed at that temperature, whereas the dependence on light intensity is $G^{0.4}$ also observed. The explanations to these observations are still debatable. The simulation studies [11] using the tight- binding molecular dynamics technique explaining the role of floating bonds and its kinetics and H-flip meta-stability has also been able to explain some observations of SW effect. Hydrogen collision model of Branz [12] explains the SW effect by studying mobile H created by recombination of photo-generated carriers and then the two mobile H associating to form a meta-stable two-H complex and two dangling bonds in a metastable state for undoped a-Si:H.

Yang and Chen [13] showed fast and slow metastable defects using two step light soaking at high and low intensities. Recently Stephan Heck [14], Paul Stradins [15] and C Wronski [16] showed that two types of defects existed and could be seen in mobility-lifetime Vs alpha studies during annealing of films after light induced degradation as both the defects had different annealing energies. Although they found two types of defects during annealing, the plot of α Vs $(\mu\tau)^{-1}$ showed a straight line during the exposure. The goal of this research is to find the fast defects during light exposure. It is believed that if the defects can be seen during the annealing, these defects should also be created at different rates during degradation and need to be found out.

With this overview we now go further into the details of this problem and the past studies done trying to explain the problem.

CHAPTER 2

LITERATURE REVIEW

Ever since the knowledge of Staebler–Wronski effect in 1977 [1], amorphous silicon (a-Si) as a material and hence the solar cells [17] have continued to show improvements in both the efficiency and stability as a consequence of rigorous efforts in understanding of the material characteristics. Light induced degradation kinetics has been studied intensively and lot of explanations have been put forward, some of them that have been widely accepted and worked upon have been discussed in this chapter.

In the devices, breaking of the weak Si-Si bonds and the relative ease of diffusive motion of hydrogen, metastable dangling bonds can be created in addition to the initially present dangling bond density. This effect is known as the Staebler–Wronski effect. The creation of metastable defects is driven by the release of energy due to electron-hole recombination events, and is thus enhanced by illumination of the material. In a solar cell, defect creation can also be provoked in the dark by bipolar current injection in the diode. The increased dangling bond density reduces the electric field within the intrinsic part of the diode and enhances the recombination losses in the cell, by which the cell performance deteriorates. If a pin cell is made thin (<250 nm), it does not show significant deterioration induced by SWE because the drift-assisted charge-carrier collection length does not degrade to values below the cell thickness, even though metastable dangling bonds are still created. But for achieving considerable absorption films of around ~1 μm thick are required where the SWE effect plays significant role.

In the films too, the photoconductivity and dark conductivity of the undoped a-Si: H is observed to decrease with light exposure. These light induced defects are observed to be reversible in a way that the original properties of the films could be restored, by annealing at 200°C in dark. Staebler and Wronski hypothesized that this meta-stability might be associated with trapping of photo-generated carriers at defect sites, or the movement of hydrogen atoms and micro-void formation. To study the origins of these induced defects, careful studies on the structures of defects has been carried out. The light induced

degradation of the optoelectronic properties of a-Si: H is observed to be accompanied by an increase in the concentration of the paramagnetic centers. The characteristics of the electron spin resonance (ESR) for these defects are very similar to the intrinsic defects of the annealed a-Si: H. Despite this similarity differences do exist in the line shape of the transient light induced ESR signals, indicating that the local environment of the light induced defects is somewhat different from those of intrinsic defects. The increase of metastable defects has also been detected through the increase in sub band-gap absorption. The concentration of light induced defects has been demonstrated to increase with doping level and high level of impurities like the presence of Germanium, Carbon, and Oxygen in a-Si alloys [19, 20]. Currently, many investigators agree that the dangling bond created by light soaking can exist in three different charge states located differently in the band-gap (D^+, D^0, and D^-) as shown in Figure [2.1]. These states act as recombination centers which deteriorate the material quality and degrade the solar cell performance. Even in films of very low impurities the SWE still persists indicating that the impurities are not the culprit in high quality a-Si alloys.

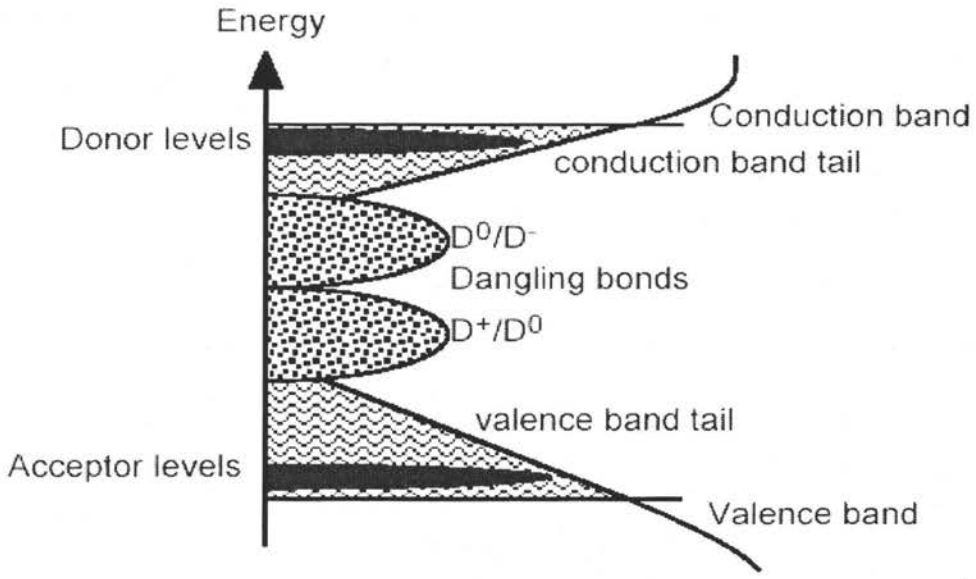

Figure 2.1: Different types of defects in forbidden gap between conduction and valence band tail states.

The studies of the kinetics of these metastable defects densities (N_D) show that N_D increases with both the illumination density (G) and exposure time through the relationship:

$$N_D \cong k.G^{2/3}t^{1/3} \qquad (2.1)$$

In deriving this expression it is assumed that the defect creation rate is proportional to the recombination rate and that the carrier density at the band edges is proportional to $\frac{G}{N_d}$. It is interesting to know that these studies demonstrate that the defect creation process is to a great extent independent of the temperature over a wide range from $4.2K$ to $300K$ [21]. The creation of light-induced defects causes changes in optical and electrical transport properties of a-Si: H and alloys; the extended state electron mobility, the electron lifetime and the electron and hole diffusion length are among these. However it is observed that while the degradation of photoconductivity and the electron diffusion length correlates with the increase in the density of metastable defects, hole diffusion length remains constant for short exposure time before eventually starting to decrease. These are the evidences that the degradation mechanism has not totally been understood yet.

There is clear evidence that the concentration of metastable defects in a-Si: H saturates at around 10^{17} cm^{-3} after the material has been exposed to light (1 Sun) for about 1000 hr at room temperature. This condition has taken as the bench mark condition for comparing the stable efficiency of a-Si solar cells. The saturation occurs at low temperatures, so it's not simply the result of thermal annealing. In physical terms, the processes that control degradation are speeded up by high intensities, so that changes occur in shorter times.

One important observation from the study of the defect densities is that the saturated defect density N_d is weakly dependent on the intensity. This is because when saturation, i.e., steady state, is reached, the rate of light-induced degradation is just offset by the light induced recovery. The value that N_d takes is just a fraction of the total number of centers in the material that can be converted to defects. It is observed that any difference in optical

properties of material may alter the rate of degradation independent of the saturation density of defects.

Some researchers have tried to overcome SWE replacing hydrogen by deuterium [22]. Researchers have carried out some experiments on using SiD4 and D2 gases and observed that the deuterated solar cells indeed showed an improved stability against light soaking over their hydrogenated counterparts, though SWE not totally eliminated. Ion Mass Spectroscopy analysis results that on the deuterated cell still a hydrogen concentration of 10^{20}/cc exists, which probably originate from the reactor walls or the source gases. Since metastable defect density is less than this, the possibility that the residual hydrogen maybe responsible for degradation cannot be ruled out. There have been few models which try to analyze and explain the kinetics of light induced degradation which have been briefly discussed here.

1. Trap to Dangling Bond Conversion Model:

The essence of this model which was first proposed by Adler [23] and later quantified by Dalal [24] was that in equilibrium there are always lots of silicon DB's, most of which exist in positive or negative charge states and are not seen by ESR. Under the optical excitation these defects capture photo excited carriers, and thus convert into neutral, rehybridized condition that is the paramagnetic stable state. Thus carrier capture by the hypothesized charge defects is central to the formation of the metastable state. Adler had proposed based on evidence from Reimer et al [25] that a-Si: H films are inhomogeneous, consisting of regions of high and low concentrations of hydrogen and potential fluctuations, due to clustered and dilute Hydrogen which may be responsible for the charged states (D^+ and D^-) and isolated D^0 states. The model deals with the conversion of existing DB defects under illumination and not formation of new ones. It assumes the photo-generated carriers can be trapped by the isolated D^0 centers via the following processes

$$D^0 + e^- \rightarrow D^- \tag{2.2}$$

$$D^0 + h^+ \rightarrow D^+ \tag{2.3}$$

Adler assumed that the defects have a negative correlation energy (U<0) so there neutral state doesn't occur in equilibrium. These D^+ and D^- pairs represent the vast majority of charged gap states and can act as relatively shallow traps via the following reactions

$$D^+ + e^- \rightarrow D^0 \tag{2.4}$$

and hence act as very effective recombination centers. Adler considers that the above reactions would induce a shift in the effective density of states, increasing the density of D^0 centers which are induced by free career recombination as been shown in Figure [2.2], where T_3^0, $T_3^+$and $T_3^-$are neutral, positive and negatively charged dangling bonds.

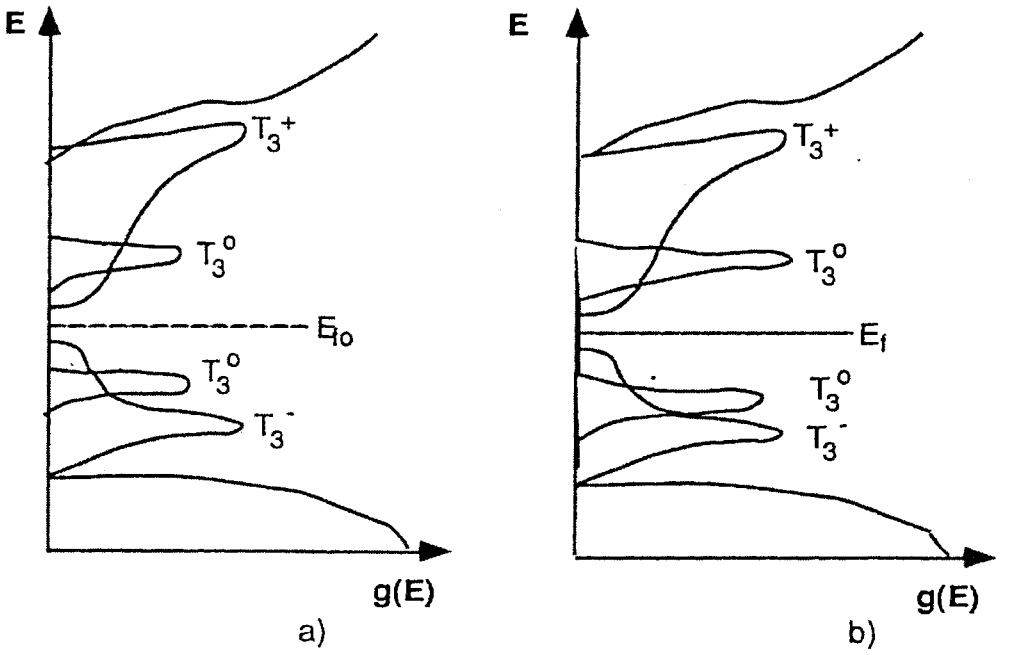

Figure 2.2: Effective one electron DOS for a-Si:H (a) equilibrium state (b) light soaked state [23]

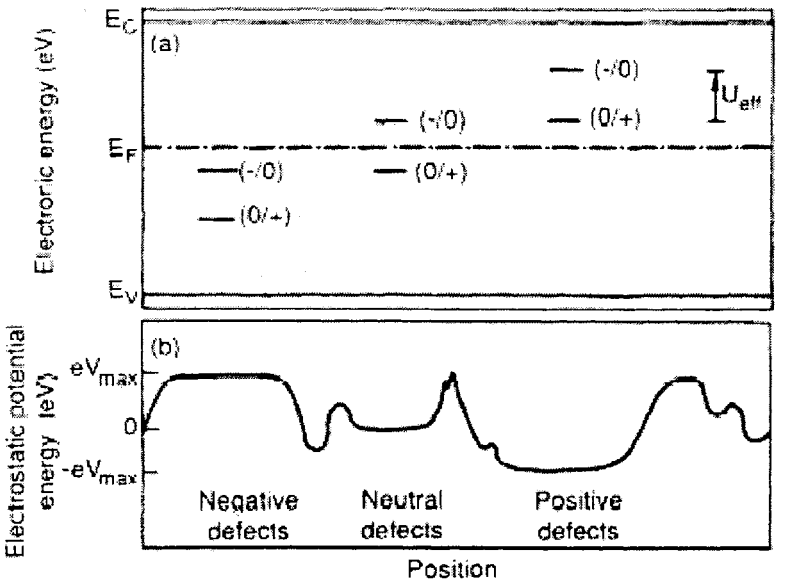

Figure 2.3: A random electrostatic potential and its effect on transition levels of the dangling bond defect [26]

More recently Branz and Silver [26] have shown the existence of these defects and have related them to local potential fluctuations as shown in the Figure [2.3]. They have shown the (0/+) transition taking place with positive effective correlation energy.

The Figure [2.4] shows the trap quasi Fermi energies separating the traps from the recombination centers depending on their position as given by Simmons and Taylor [45], where b_n and b_p are the capture rate coefficients for the electrons and holes respectively. Because $b_n / b_p << 1$ for a (- / 0) level, a (- / 0) anywhere in the lower half of the gap is likely to act as a hole trap. Near and above mid-gap, a (- / 0 level functions as a recombination center. For a small range near the conduction band edge, (- / 0) acts as an electron trap. The other half of the Figure is for (0 / +) transitions.

The goal of this research is to look for the negative defects in both doped and undoped a-Si: H and see what transitions are taking place at various energy levels when the films are exposed to light. If true this would supports the Adler's model as explained above. Adler also proposed that annealing of these neutral states formed restores the ground states

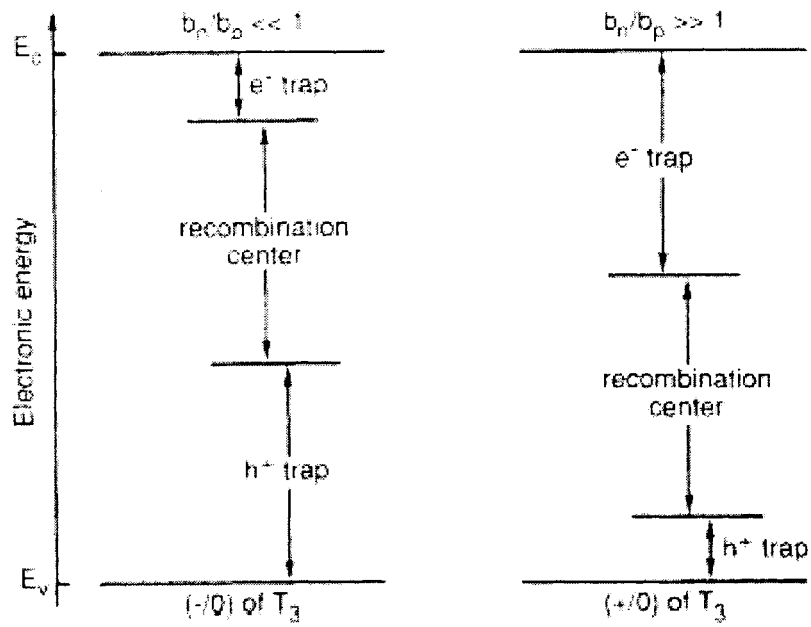

Figure 2.4: Schematic diagram of the trap-quasi Fermi energies dividing traps from the recombination center [26]

of D^+ and D^- in their respective hybridization states of low and high potential and hence the above is a metastable state.

2. Weak Bond Breaking Model:

This model has been the most popular explanation of formation of metastable defects among researchers.

Pankove and Berkeyheiser (7) first suggested that light induced defects are formed by breaking of weak Si-Si bonds, and the broken bonds provide non-radiative recombination paths for carriers as shown in Figure [2.5]. Fathallah [27] showed that the defects can even be formed by excitation with light with photon energy of 1 eV and even $\leq$ 1 eV because of the movement of the levels in the gap, though the strength of Si-Si bond is about 2.2 eV. The degradation of optically detected magnetic resonance observed by Morigaki [28] was also attributed to formation of DB centers by light and the increase and decrease in strength of ESR line at g= 2.0055 upon exposure or annealing was sign of Si dangling bonds.

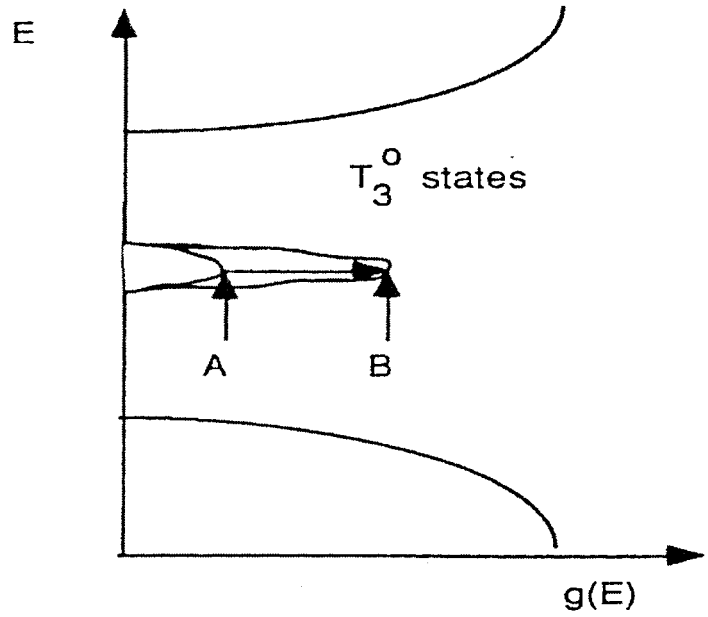

Figure 2.5: Schematic of bond breaking model showing the DOS for a-Si:H upon exposure, A is the annealed and B is light soaked state [23].

3. Two Defect Model:

Upon illumination two different mechanisms may take place which will result in two different types of defects which can be clearly seen with sub-band gap measurements.

Han and Fritzsche [29] first discovered that the photoconductivity in a-Si:H is not a single valued function of DB density. At the same DB density, σ_{ph} can be an order of magnitude lower during light soaking than during subsequent annealing. It was proposed that one of the two types of defects causes most of the light induced decrease in σ_{ph}, and the other responsible for the increase in sub-gap absorption. However it had been difficult to confirm that there are really two types of defects rather than one defect with a distribution of annealing energies and recombination properties.

Recently Stephan Heck, Paul Stradins and C Wronski [14, 15, and 16] showed that these two types of defects existed and could be seen during annealing of films after light induced degradation as both the defects had different annealing energies as shown in the

Figure [2.6] below. This is a plot of $\alpha_{1.3}$ Vs $(\mu\tau)^{-1}$ as both increase with light exposure and decrease during step-wise isochronal anneal. The plot confirms the fast and slow components of the annealing curve. Up to 110^0 C, $(\mu\tau)^{-1}$ recovers fast, while $\alpha_{1.3}$ remains nearly constant. At 130^0 C and above, $(\mu\tau)^{-1}$ recovers more slowly and falls almost linearly with $\alpha_{1.3}$.

Figure [2.7] shows $\alpha_{1.1}$ is graphed versus $\alpha_{1.3}$ for the same experiment as Figure [2.6], this time the data is normalized to annealed values before degradation. There is an increase of $\alpha_{1.1}$ of about 30% with respect to its degraded value, before $\alpha_{1.1}$ decreases linearly with $\alpha_{1.24}$ to its annealed value. This transition occurs at the same T= 110 C at which $\alpha_{1.1}$ changes from fast to slow recovery as shown in Figure [2.8]. They named the fast annealing defects as Primary Recombination "pr" centers which differ from DB defects. The three finger prints of pr center annealing which appear at temperatures too low for DB annealing are: 1.) an anneal activation energy of 0.85 eV (2.) a sharp increase in photoconductivity (3.) increase in hυ ≤1.1 eV optical absorption

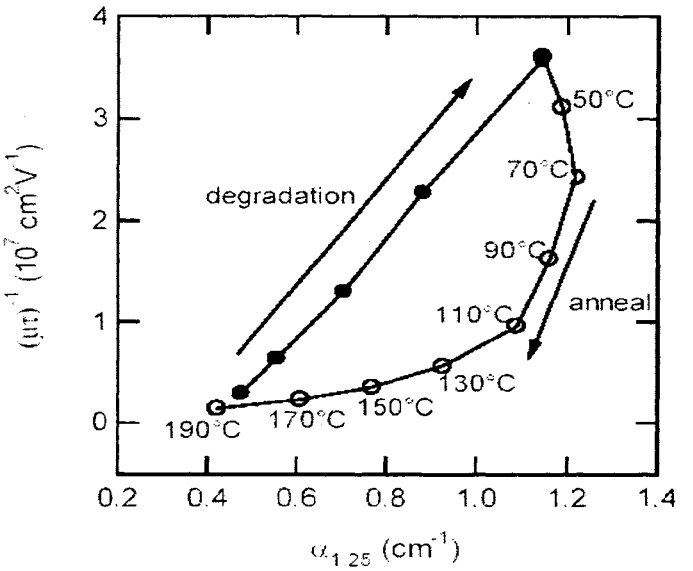

Figure 2.6: μτ Vs α for degradation and isochronal step-wise annealing curves showing two different defects with different annealing energies[14].

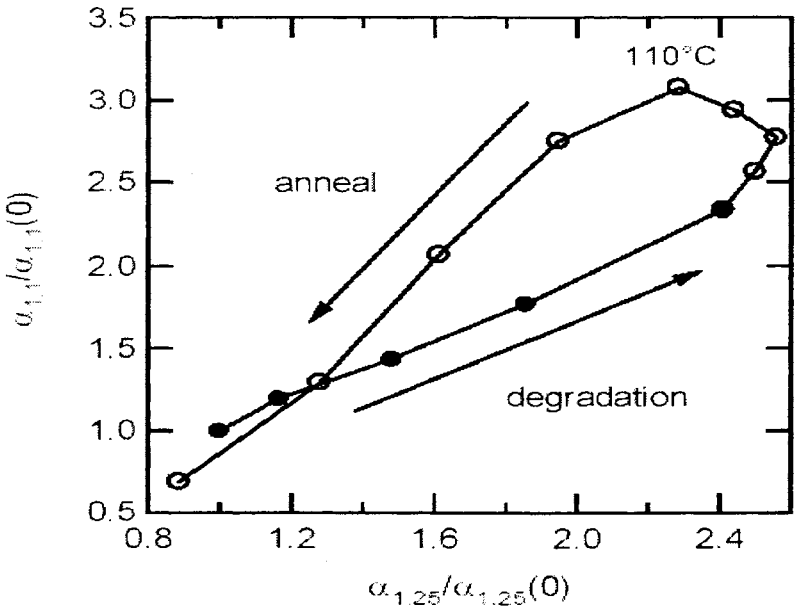

Figure 2.7: $\alpha_{1.1}$ *Vs,* $\alpha_{1.25}$ *the same for which previous plot was made [14].*

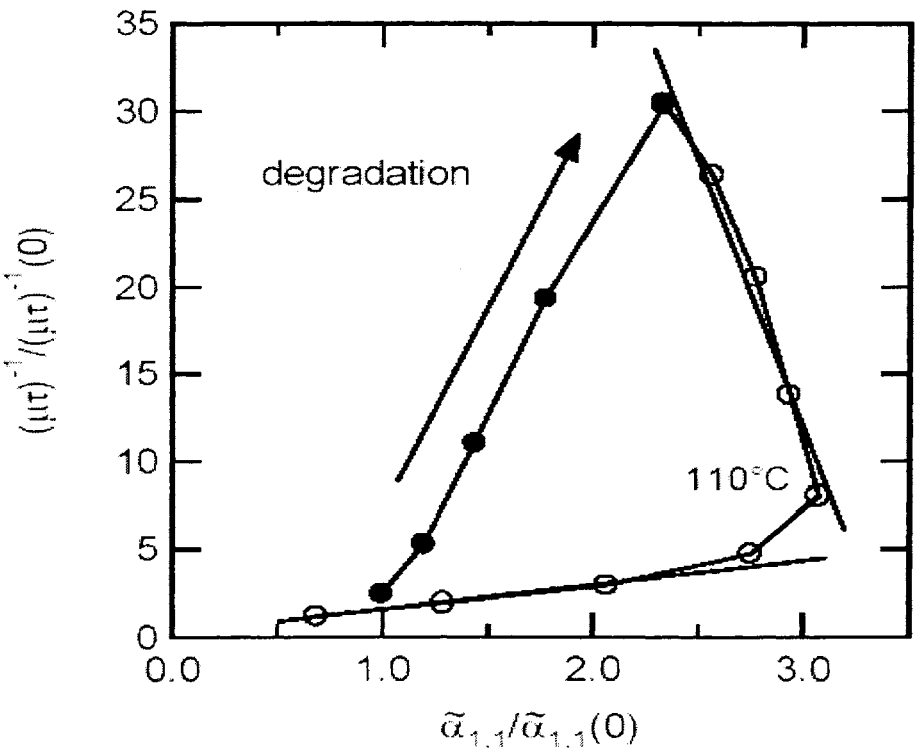

F igure 2.8: Normalized $(\mu\tau)^{-1}$ *Vs absorption* $\alpha_{1.1}$*, during degradation and 30 min stepwise anneals [14]*

CHAPTER 3

MATERIAL GROWTH AND CHARACTERIZATION

Sample Preparation:

All the a-Si: H films were made in ECR-PECVD reactor used for the deposition of the films on the Corning 7059 glass. The samples were cleaned by the standard UV treatment. First the samples were boiled in acetone for 10 minutes, followed by a 10 minutes of standard UV cleaning in methanol. These cleaned samples were then stored in methanol and dried by nitrogen just before being loaded.

The unique features of ECR plasma make it superior to other conventional methods of deposition. The details of the reactor in MRC and chemistry behind the growth of films can be learnt from many of the papers from our group [31].

In the ECR PECVD system, the dissociation of the feed-stock gases which is basically SiH_4 and H_2 by the plasma may lead to different radicals and lots can be learned from standard model of a-Si: H growth according to Matsuda [33], Perrin [34], and Gallagher [35] (MGP model) and V Dalal [32,36]. The H dilution plays a very significant role in passivating the defects and hence decreasing the density of DB defects by several orders of magnitude. Increasing the H content leads to increasing band gap, with the Tauc bandgap varying from ~1.7 eV to 1.95 eV as the deposition temperature is reduced and H content is increased from the normal 6-8 % to 10-15%.

Characterization Techniques

1. Thickness

The thickness of the films was determined from the period of oscillations in the transmission versus wavelength curve in the 1000 to 2500 nm range by using the equation

$$t = \frac{i}{2n\Delta(\frac{1}{\lambda})} \tag{3.1}$$

$$\text{where } \frac{1}{\lambda} = \frac{1}{\lambda_1} - \frac{1}{\lambda_2} \tag{3.2}$$

where i is the number of complete cycles from $\lambda_1$to λ_2 which are the wavelengths of the i cycles. For the two adjacent maxima or minima, i =1. Figure [3.1] shows the signature transmission of films which can be used to extract the thickness

n_1 is the index of refraction and is usually 3.6 for the a-Si:H films over the above wavelength range. It is also possible to acquire a more accurate value for the index of refraction by obtaining the reflection spectra of the film and solving for n_1 in the expression

$$Avg(R) = \frac{(n_1 - n_0)^2}{(n_1 + n_0)^2} \tag{3.3}$$

Where Avg (R) is the average reflection in the non-absorbing range

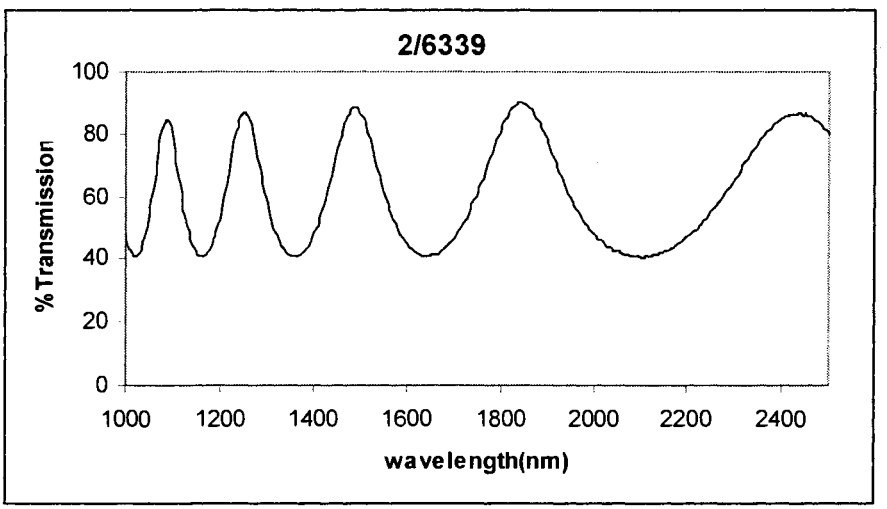

Figure 3.1: Plot of % Transmission Vs Wavelength obtained from Lamda-9 spectrophotometer

2. Photo and dark conductivity

When the semiconductor is in thermal equilibrium the hole and electron carrier concentration is balanced by thermal generation and recombination processes. These free carriers lead to conductivity in the material and are related as

$$\sigma = qn_0\mu_n + qp_0\mu_p \tag{3.4}$$

$$\sigma_{n,p} = \sigma_0 \frac{\exp-(E_{c,v} - E_{fn,p})}{kT} \tag{3.5}$$

where n_0, p_0 are the concentrations of electrons and holes respectively while μ_n, μ_p are their respective mobilities. The equation [3.5] gives us an estimate of the position of the Fermi Level at a given temperature T from Fermi statistics. The equation has $E_{c,v}$ which is the conduction or valence band edge defined by mobility gap, $E_{fn,p}$ is the quasi Fermi Level and σ_0 is the conductivity pre-factor known as minimum metallic conductivity.

Photoconductivity occurs when carriers are optically excited from non-conducting to conducting states. It relates to the photo generation, transport and recombination of electrons and holes. This illumination excites the electrons and holes to the band edges where they drift toward electrodes under the applied field. This conductivity when normalized against the actual amount of light absorption is equal to the product of quantum efficiency, mobility and recombination life time ($\eta\mu t$) for majority carriers.

Photosensitivity is defined as the ratio of photo and dark conductivity at room temperature. The good value of photosensitivity is around $\sim 10^5$ which signify good quality film. In the set up an external voltage of 100V was applied under 1.5 Air-mass (AMS) lamp. The equation used is

$$\sigma_{l,d} = \frac{L}{W}.(\frac{I}{V.d}) \tag{3.6}$$

where L / W is the length to width ratio of the metal contact, d is the thickness of the film and V is applied voltage and I is the photocurrent. Carriers in good films have less probability of getting trapped as they have low defects, and hence the photoconductivity is large.

3. Activation Energy

Activation Energy is a measure of conductivity due to thermal excitation versus temperature. In amorphous semiconductors like a-Si: H activation energy E_a gives us indication of how intrinsic is the material and is basically difference between the conduction band and the Fermi level. Thus it can be used to assess the presence of impurities, either intentional (B or P dopant atoms), or unintentional (O or N), the Fermi level shifts over several tenths of eV towards the conduction or valence band accordingly. The activation energy is determined from log σ (T) versus 1/T plot Figure [3.2], with $140 < T < 200^0$ C. For undoped material E_a is about 0.8-0.85 eV. The Fermi level is at mid-gap position, as typically E_g ~1.6-1.7 eV.

$$\sigma = \sigma_0 \exp(-\frac{E_a}{kT}) \tag{3.7}$$

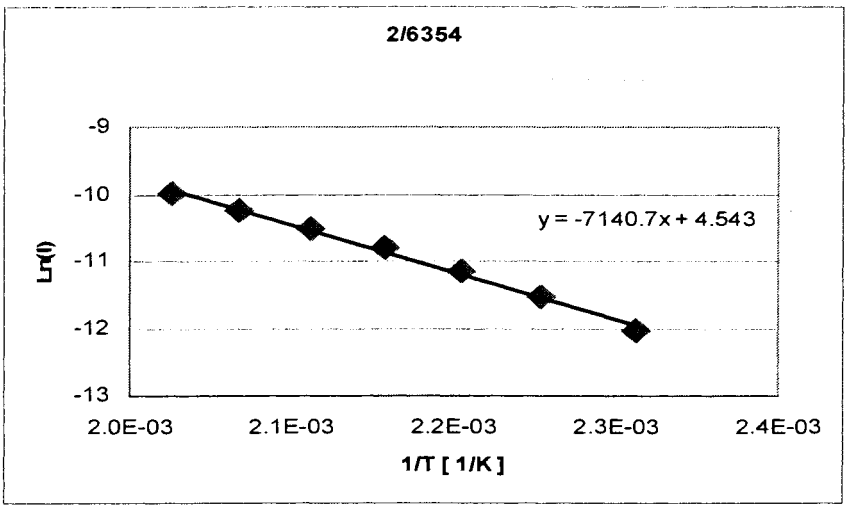

Figure 3.2: Plot of ln (I) Vs $\frac{1}{T}$ *used to measure Activation Energy*

In this setup, the substrate is placed on a heater block inside a light tight box to eliminate carrier excitation due to photon absorption. The temperature is not allowed above 200 C to prevent reordering of the film. A 100V bias is placed across the contacts to enhance the current.

4. Optical Absorption:

The optical absorption occurs when the incident photons of light falling on sample make the electrons gain enough energy to move from the valence band into the conduction band. The optical properties of the material are defined by the spectral dependence of its complex index of refraction,

$$\varepsilon_r = n(E) = ik(E) \tag{3.8}$$

where n is the refractive index and k is the absorption index. The spectral region of major interest is in the vicinity of the absorption edge, since it provides information about the band gap and the density of states within the gap. For semiconductors such as a-Si:H, n and k are usually determined from the reflection (R) and transmission measurements as shown by Heavens [37]. In the absorption curve there are three regions of interest.

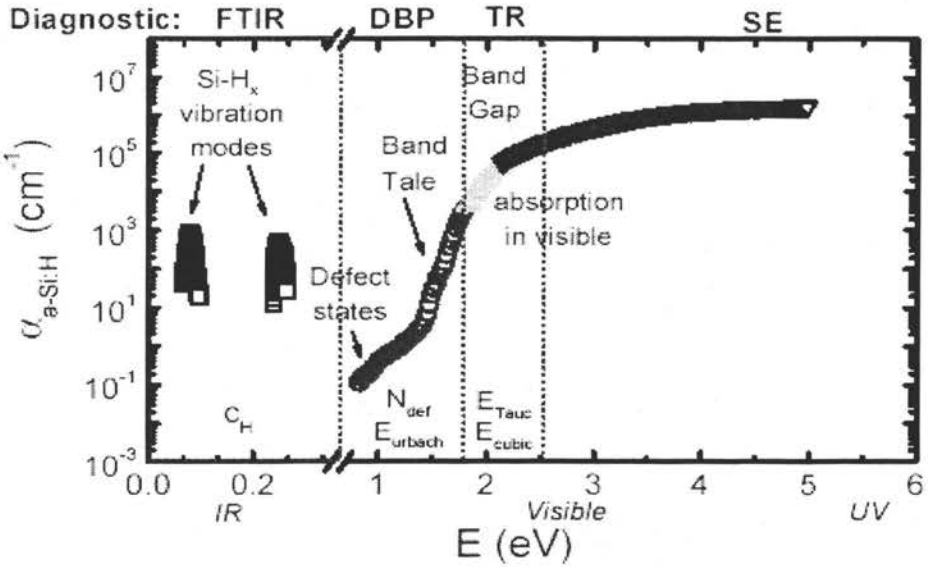

Figure 3.3: The α Vs E for a-Si:H at different energies [44]

One of the regions is the region of high absorption as shown in Figure [3.3]. For the absorption coefficient larger than 10^3 cm^{-1}, absorption takes place between extended states. In crystalline materials it involves both direct and indirect transitions which involve the absorption of an electromagnetic wave by an electron in the valence band that is then raised to the conduction band. However indirect transitions involve the interaction with the phonons.

Since amorphous silicon is a direct band gap material the absorption coefficient α is given by

$$\alpha n_1 h\omega = B(h\omega - E_g)^n \tag{3.9}$$

where n = 2 or 3, depending on whether the transition is quantum mechanically allowed or forbidden. The pre-factor B for amorphous semiconductors is given by properties of the material and is given by Mott and Davis [38]

$$B = \frac{4\pi\sigma_{min}}{n_1 c \Delta E_w} \tag{3.10}$$

where σ_{min} is the minimum metallic conductivity, c is the velocity of the light and ΔE_w is the extent of band tailing. The equation above is used to deduce the optical band gap energy also called 'Tauc Energy' [39]. E_{tauc} can be determined by plotting ($\alpha h\omega$) as a function of $h\omega$, the incident energy of photons as shown in Figure [3.4]. This plot yields a straight line which can be extrapolated to the x-axis to determine the Tauc-Gap. Amorphous silicon usually has a value of 1.65 eV. In our measurements absorption on the films was done on a Perkin Elmer Lambda 9 UV / VIS / NIR spectrophotometer from 400- 900 nm range.

Another parameter used to characterize the band gap was E_{04}. The knee of the absorption curve typically occurs around $\alpha = 10^3$ to 10^4 cm^{-1} which is denoted as E_{03} or E_{04} energy gap respectively [40]. The difference between E_{04} and E_{tauc} is that the former is thickness independent. Typically there is 0.15 – 0.2 eV difference between them. The plot is shown in Figure [3.5].

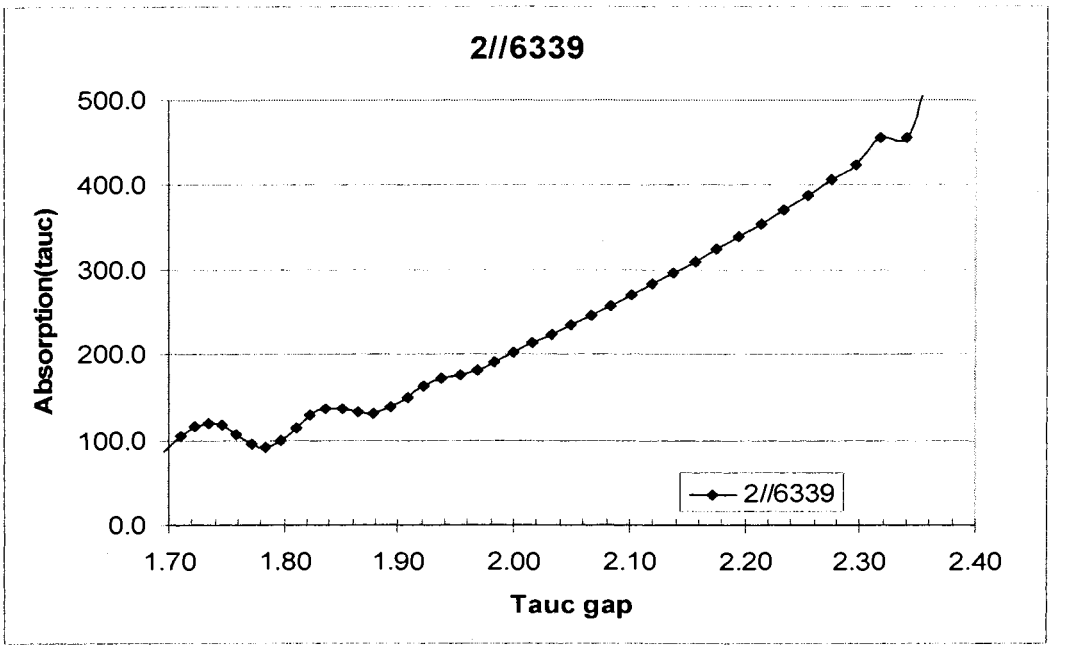

Figure 3.4- E_{tauc} Vs Energy obtained from Lamda-9 Spectrophotometer

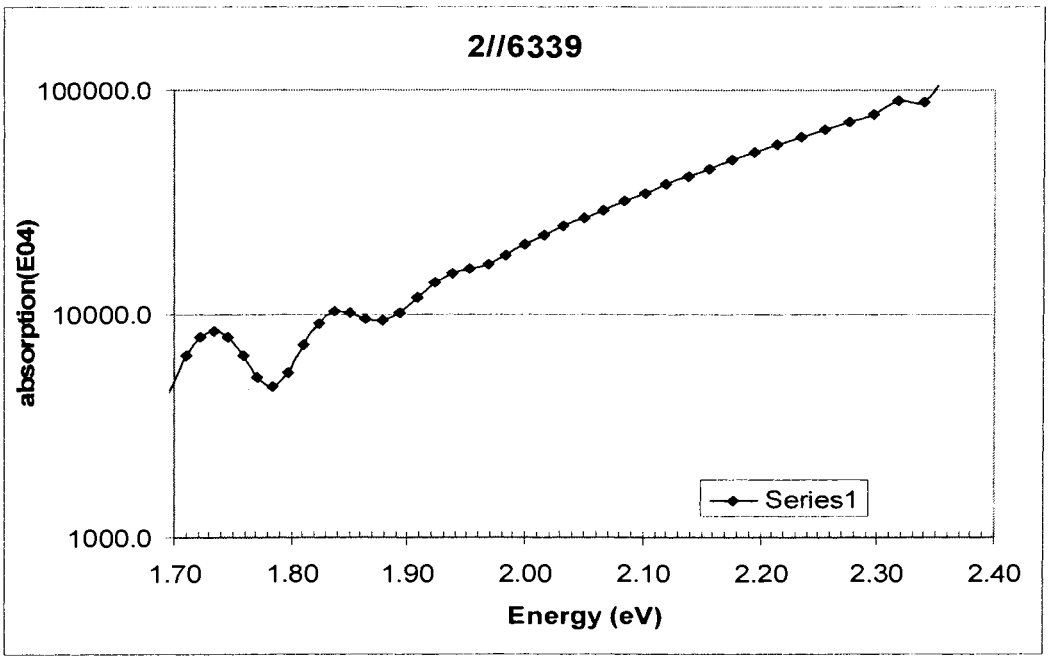

Figure 3.5: E_{04} Vs Energy obtained from Lamda-9 Spectrophotometer

In virtually all semiconductors an exponential region is observed. This is seen in the range of $1 < \alpha < 10^3$ cm^{-1} where absorption takes place between sub-band gap states.

The region is referred to as the Urbach Tail and several mechanisms have been proposed to explain it, such as band gap variations due to density fluctuations, broadening of the band edge or the presence of excitonic states induced by internal electric fields. Aljalali [41] suggested that the absorption edge reflects the tailing of the states into the gap region due to fluctuations in bond lengths and bond angles. There has been lot of other speculation about this in the literature.

This measurement gives us a lot of information about the quality of the film. The curve of absorption coefficient α vs. photon energy hv yields a joint valance band conduction band density of states, when one makes an assumption that the matrix element for absorption is independent of hv. In amorphous semiconductors like a-Si:H films which are usually thin films (~1 μm) as in our case, geometry limits the accurate determination of α from optical absorption and reflection data to $\alpha > 1000$ cm^{-1}. Thus indirect measurement techniques like photo-thermal deflection spectroscopy (PDS) and constant Photo-Current method (CPM) and Dual Beam Photoconductivity (DBP) are used to measure α around 0.1 to 10 cm^{-1}. Since the DBP technique has been widely used in our experiments, is now explained in detail.

Dual Beam Photoconductivity Method:

This technique is used to measure the sub-band gap absorption of the amorphous semiconductors. It was first developed by Wronski and his co-workers [42]. The experimental set up for this technique is shown in Figure [3.6].

In this DC beam light of (~1Amp) shines on the sample to fix the quasi Fermi levels (and hence fix carrier life times) and the small AC light measures the photoconductivity for the sample. The dc beam continuously creates electron hole pairs that keep the mid-gap states (traps) filled and keeps the occupancy of the mid-gap states unchanged.

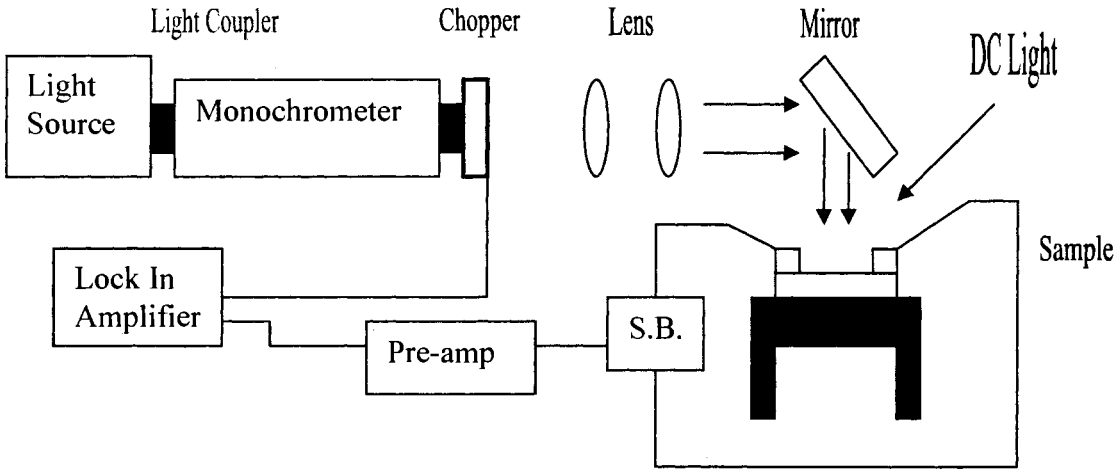

Figure 3.6: Dual Beam Photoconductivity Set up

The ac beam superimposes on the dc beam and thus modulates the photocurrent generated in a sample by creating the additional electron-hole pairs. The change in the photocurrent produced in the sample as we change the wavelength of the ac beam from the monochrometer can be detected by a lock in amplifier with signal being amplified using a pre-amplifier. This signal can be related to the absorption coefficient of the film with respect to wavelengths as the lifetimes of the carriers are constant.

The range of the monochrometer that we have used is from 600 nm to 1300 nm where the output light was chopped by chopper modulating the photon signal to produce 13.5 Hz square wave. This reduces the noise due to ambient light and 60 Hz power lines. Taking in consideration the sensitivity of the experiment, all the measurements were made with room lights off. Different high pass filters were used each at 700, 900 and 1200 nm to get rid of the lower wavelengths and to reduce second harmonics. A neutral density filter was also used in highly absorbing region (where the incident photon energy is closer to or above the band gap) to maintain the excess carrier density constant. The chopped beam is focused on the sample through the beam splitter, with the other half going to photo-detector used as reference cell. To enhance the measured signal, a bias of 9 V is applied across the sample to improve the transport of the electron-hole pairs. The absorption coefficient is calculated at

each wavelength by dividing the signal by a reference signal and then multiplying with quantum efficiency of the Si (~1100nm) and Ge (1100- 1300 nm) reference detectors. This value is then normalized to the band gap absorption value so that it can even be matched to E_{04} value. Usually good films have an Urbach energy value of around ~43 eV.

Bullot et al [43] concluded that the steady state photoconductivity is due to at least three processes:

1. electrons trapped on dangling bonds are thermally emitted into the conduction band

2. electrons trapped in the localized states of the conduction band tail are thermally emitted into the conduction band

3. holes in the valence band tail diffuse and recombine with the D- dangling bonds.

The third region can be related to intraband transitions and DOS. Usually photoelectric effects are used to measure absorption in this region like Photo thermal Deflection Spectroscopy (PDS) and Photo Acoustic Spectroscopy (PAS).

CHAPTER4

RESULTS AND DISCUSSION

Results

All the samples are a-Si: H and have been prepared in ECR PECVD reactor which has been described earlier. All the samples have been grown for the same time and almost same temperature. The pressure and power used during the deposition of the film have been shown before to produce the best quality in amorphous films in our reactor. The H_2: SiH_4 ratio was kept constant for all the samples. Though there were lot of samples made and studied for this experiment (including 2/6339, 2/6243, 2/6244, 2/6341, 2/6342) only few have been shown here for the comparison.

These samples as the Table1 shows were grown around ~380^0 C which may not be suitable temperature for growing best quality a-Si:H films. But growth at these high temperatures the SiH_2 bonds formed during the growth of the film are comparatively less which inhibit the growth of voids in films and higher temperatures also lead to breaking of the weak bonds by thermal energy hence suppressing the bond breaking in our samples during the initial degradation. The sample 2/6214 is doped a-Si: H with O used from the He:O cylinder while 2/6339 is undoped a-Si: H film with B compensation to take care of any accidental O in the film. The sample 2/6353 was made with an oxygen (air) leak and B compensation while 2/6354 has no B compensation. The last two samples were grown in same reactor conditions.

The sample films had a novel film structure with the i- layer sandwiched between two thin, larger gap a-(Si, C):H layers to guard against false results arising from the surface recombination effects. The surface a-(Si, C):H layers because of their larger band gap drive the electrons and holes away from the front and back surfaces. The higher dark conductivities are signature of O donors in the films.

Sample Parameters:

Sample No.	Time	Temp	Pressure	Power	H2	He : O	SiH4	TMB
2/6214	120	400	10	5	60	20	15	0
2/6339	120	380	10	5	60	0	15	15
2/6353	120	380	10	5	60	O leak	15	15
2/6354	120	380	10	5	60	O leak	15	0

Table 1: Growth conditions of different samples

Table2: Optical and electronic properties

Sample No	T (μm)	E 04	E Tauc	σ (photo)	σ (dark)	σ(p) / σ d)	Ea(eV)	Eu(meV)
2/6198	1.1	1.87	1.72	1.21 E-5	6.85 E-11	1.76 E+5	0.95	46
2/6214	1.18	1.88	1.71	5.21 E-5	4.44 E-10	1.17 E+5	0.80	48
2/6339	1.07	1.85	1.69	2.65 E-4	3.29 E-8	8.07 E+3	0.84	47
2/6353	1.1	1.86	1.79	4.66 E-5	6.03 E-10	7.73 E+4	0.81	49
2/6354	1.15	1.85	1.80	2.36 E-5	1.75 E-8	1.35 E+4	0.62	47

Experimental Set Up

For all the samples after deposition, chromium contacts of ~ 500 ^{0}A were put on in the evaporator. The samples were masked and chromium was evaporated at usually pressures of ~ $1*10^{-6}$ Torr and deposition rates of ~ 8- 10 A /sec. Then silver paint was applied on the top of contacts to save the contacts from pressure of probes while taking care, that silver paint is only on the contacts and not in the region between the two contacts. The sample was annealed at 200 ^{0}C for around 2 hours. Then the measurements were made at time t=0 minutes which included optical and electrical measurements (band gap, conductivity and activation energy) as described before. Then, Transient Photoconductivity of these samples was measured for first 100 seconds. The plots of the transient photoconductivity and the explanation of the results are explained ahead. Then the sample was re-annealed for few hours to anneal out all the defects created during various measurements. Then the sub gap measurement on the samples were done for t = 0 minutes.

The sample was then degraded under the Xenon Lamp (with 2 X sun intensity). The a-(Si, C): H filter was used to allow only red photons to pass through it. The substrate holder was water cooled so as to act as a heat sink. The temperature of the substrate was measured at different stages of sample degradation by attaching a thermocouple to it for 50 hrs. The temperature remained almost constant around 32^0 C with a change of $\pm$ 0.5^0 C. The samples were degraded for different times like 0 min, 2 min, 10 min, 30 min, 2 hr, 10 hrs, 25 hrs and 50 hrs. The photoconductivity Figure [4.1] and sub gap absorption using DBP method, measurements were made at each stage for comparison and studying the kinetics of degradation. After 50 hrs when the sample approaches the saturation stage, the samples were annealed at 100^0 C for 3 min, 10 min, 30 min, 2 hrs, 5 hrs and 10 hrs. After that the samples were annealed at 200^0 C.

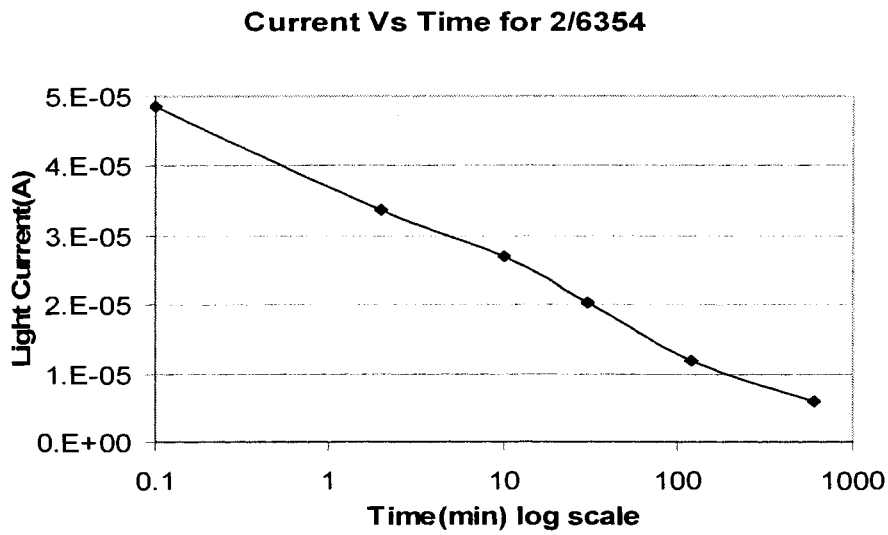

Figure 4.1: Decay in photocurrent as the sample is degraded with time

In the Figure [4.2] below, we see sub gap absorption of the undoped a-Si: H film (2/6339) with a little (ppm amount) of boron added to compensate for the accidental oxygen doping. The film was measured for the sub gap absorption at time t = 0 from 1 to 2.9 eV band gap absorption. Then the absorption was measured at t = 2 min. The plot doesn't show a significant change in the absorption curves after degradation at time t=2 min but the expanded version as shown in Figure [4.3] shows an interesting change in the pattern of the curve with a little drop around ~1.3 eV and some increase around ~1.1 eV. This can be explained by the conversion of charged states into the neutral states by the absorption of energy and hence showing an increase in absorption below the Fermi level. The sub gap absorption plots for the higher exposure times showed the weak bond breaking model coming into picture and the absorption increasing showing the overall increase in the neutral dangling bonds. Hence the initial degradation is showing something which has not been seen before, which is the conversion of the negatively charged dangling bonds into neutral bonds. To further study these changes, the next three film plots are from O doped samples which would increase the charged dangling bonds in the films.

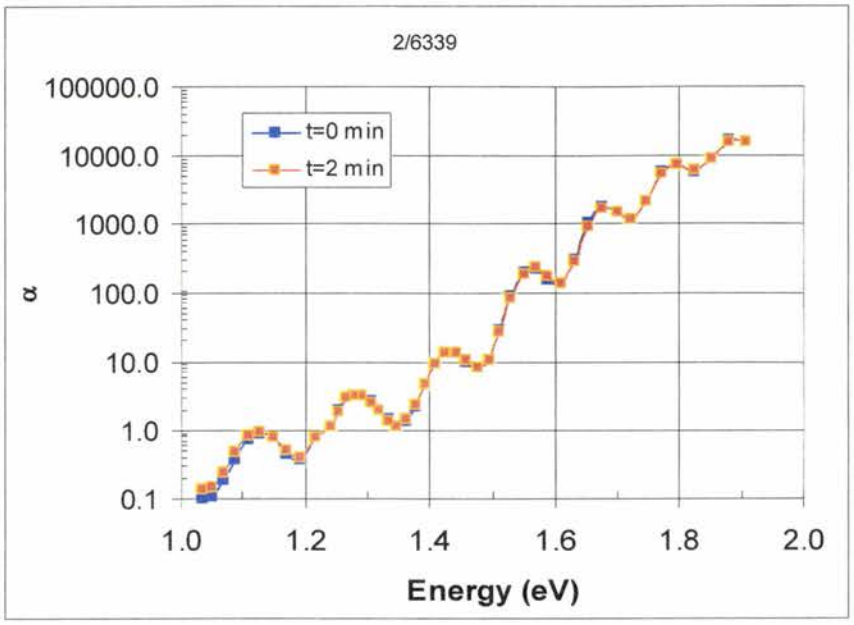

Figure 4.2: Sub-gap absorption of undoped film (2/6339) at two degradation times.

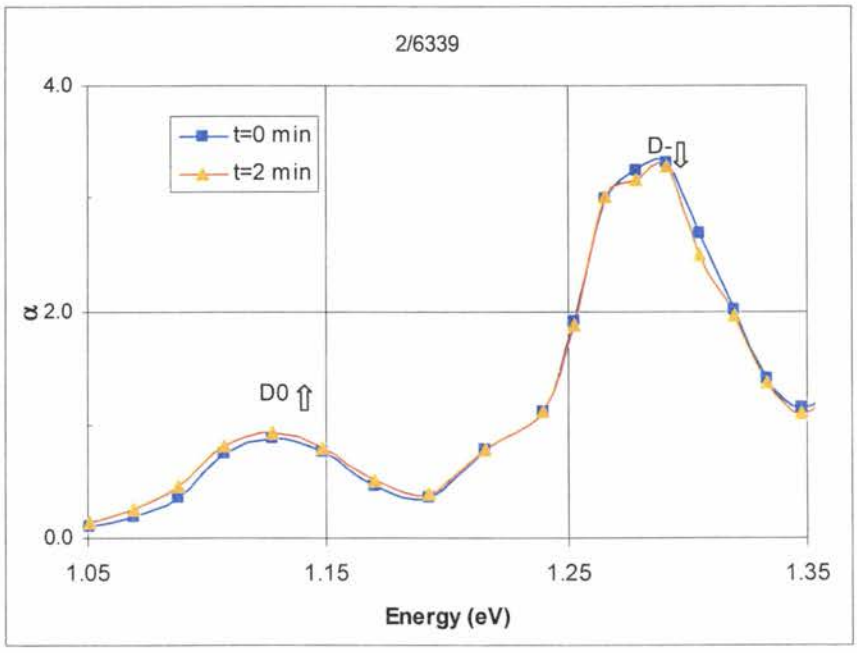

Figure 4.3: Sub-Gap plot showing changes in charged and defect states after degradation

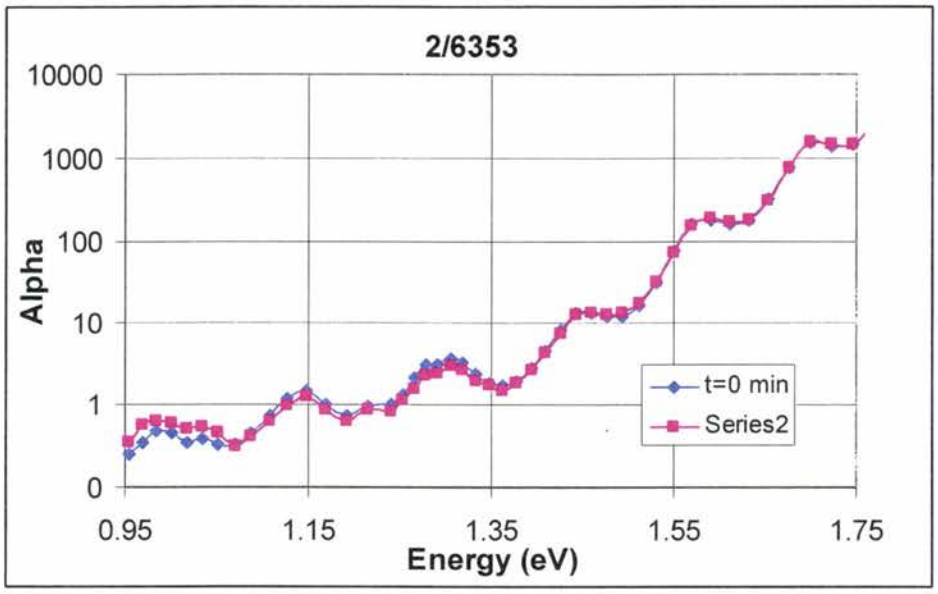

Figure 4.4: Sub-Gap Curve for an O-doped film at time = 0 and 2 minutes

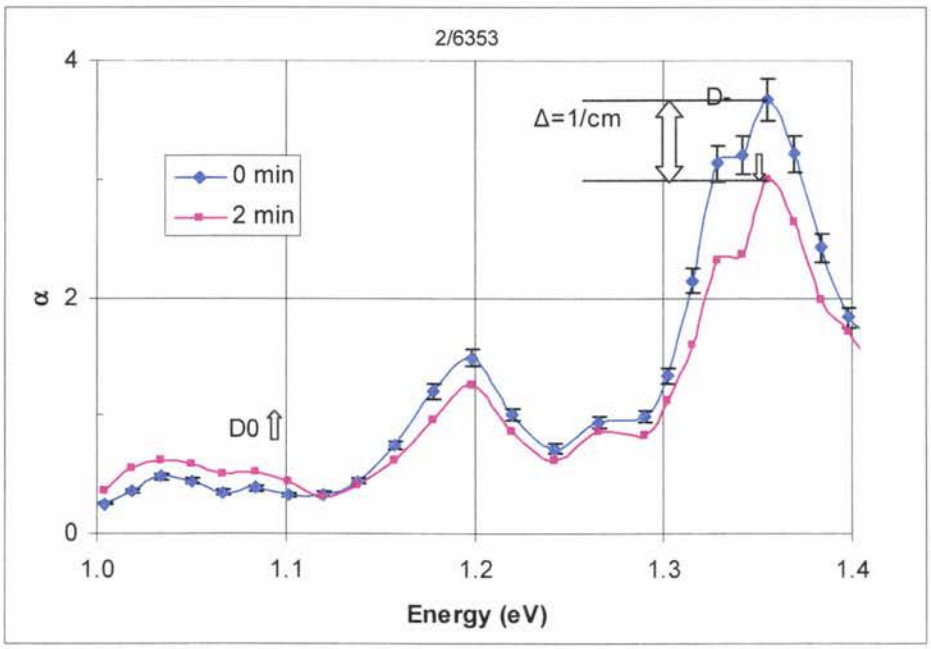

Figure 4.5: Sub-Gap plot showing the change in 2/6353

In this sample 2/6353, an air leak was introduced into the deposition chamber for some atmospheric oxygen to grow with the film. The air leak changed the pressure of the deposition chamber from 3x 10^{-7} to 2x 10^{-6} Torr. The resulting film as seen in the electronic and optical properties chart is n- doped as indicated by smaller activation energy and higher photoconductivity. This is to be expected as the activation energy which is the measure of difference between the conduction band and the Fermi Level is smaller, leading to more electrons reaching the conduction band for a given intensity of light shining on the sample. The Figure [4.4] and [4.5] clearly shows the decrease of absorption at ~ 1.3 eV and a corresponding increase at ~ 1.1 eV.

In this sample 2/6354, some donor and D^- states have been introduced by an air leak during the deposition and no addition of boron to compensate for any oxygen (ppm). The valve was open at the same position as the previous sample but the lack of boron as dopant has increased the number of D^- states. The further decrease in activation energy as compared to the last sample also shows the increase in density of the donor states. The Figure [4.6] shows this change which has been shown more clearly in the next Figure [4.7].

For this sample there is around 40% decrease in absorption ~ 1.3 eV and around 60% increase at ~ 1.1 eV. Thus these samples clearly imply a *change in the shape of the curve after light soaking.* This clearly shows that all the D^- states which are around 1.3 -1.4 eV below the conduction band in the forbidden gap have been converted into neutral dangling bonds (D^0).

All these plots show the change is around 60% increase in neutral dangling bonds which is far greater than any noise in the system during the measurement and easily covering any human errors while measurement as shown by the error bars along the points. These error bars are 5% on either side of the measured readings covering for setup, light intensity and sample position. The changes seen in these plots are significantly higher than these bars showing the magnitude of changes taking place.

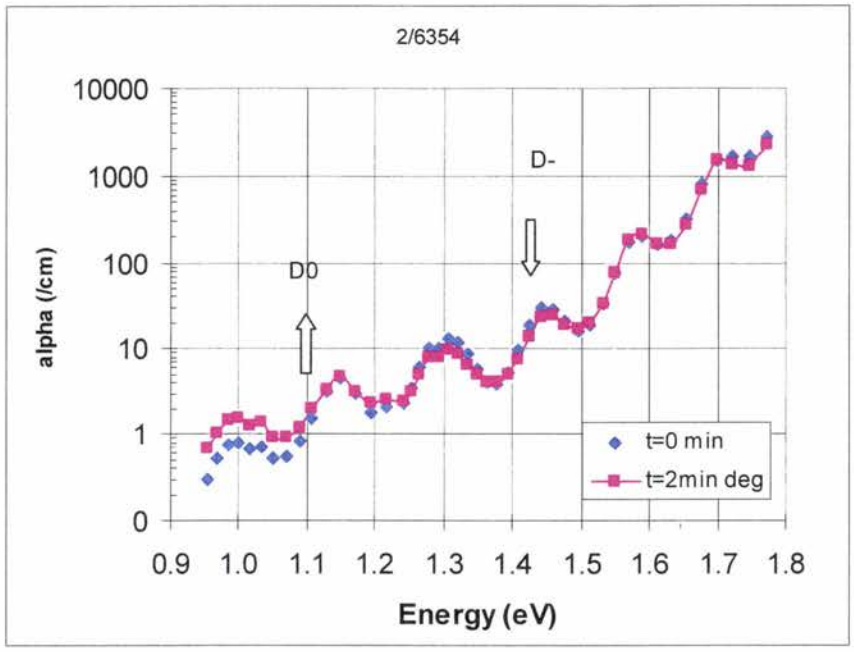

Figure 4.6: Sub-Gap Absorption curve for another O-doped sample (2/6354).

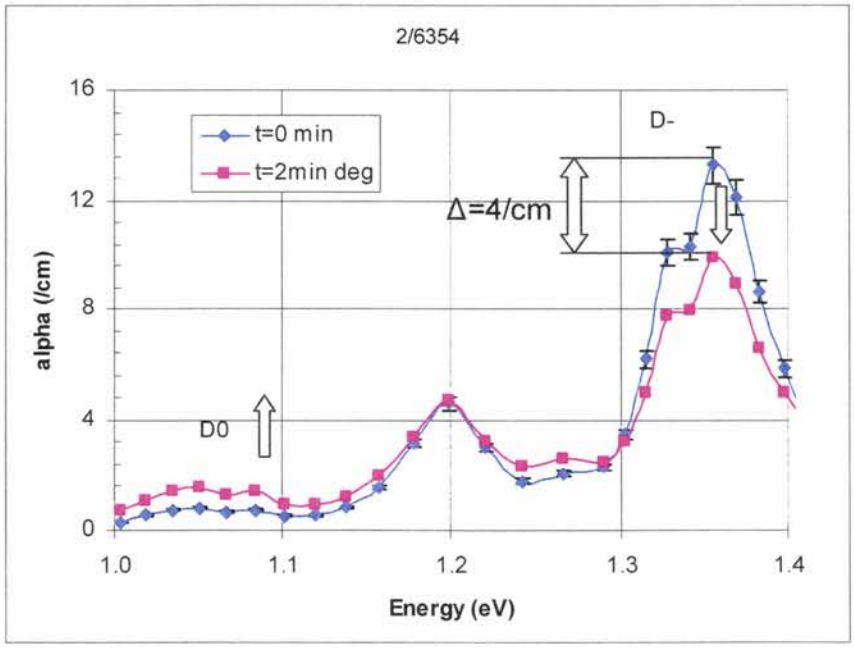

Figure 4.7: Absorption at and around 1.1 and 1.3 eV for 2/6354

These changes clearly showed the addition of donor states have increased the D-states which are finally converted into neutral states during early degradation. To prove this point further that it's the effect of O from the air leak, an O doped amorphous silicon sample was made with pure O_2 from oxygen cylinder (20 sccm of He:O mixture) to verify that this effect seen is only due to oxygen and no other impurity. Thus few samples including 2/6214 were prepared using the above conditions and the results are plotted below in the Figure [4.8, 4.9].

This also shows that both the states have negative correlation energy as proposed by Adler. Based on the bond breaking model upon illumination, the density of mid-gap states would increase due to breakage of weak Si-Si bonds and poor H bonding. It also considers that D^0 centers and does not account for the charged defects. So the measurement of sub-gap photoconductivity of a-Si: H film, it will always increase upon illumination due to larger number of band gap states irrespective of time and intensity.

But based on Adler's model which takes both the charged and neutral dangling bonds into account, charge carriers are captured by these defects and trap to dangling bond condition is invoked.

The negatively correlated state in particular is likely to be the major defect as it arises from the donor states such as oxygen which are invariably present in the films. Thus the experimental data above fits perfectly into the Adler's model and confirms that normally in undoped a-Si: H both neutral and negatively charged dangling bonds exist and contribute in SW effect.

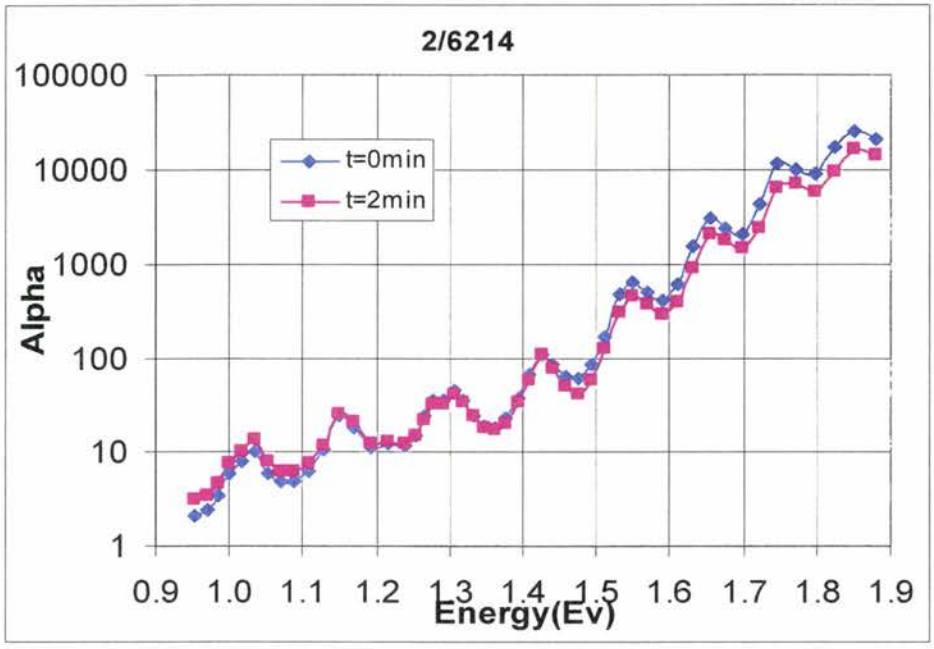

Figure 4.8: Sub-Gap Absorption of sample from Oxygen- Helium mixture.

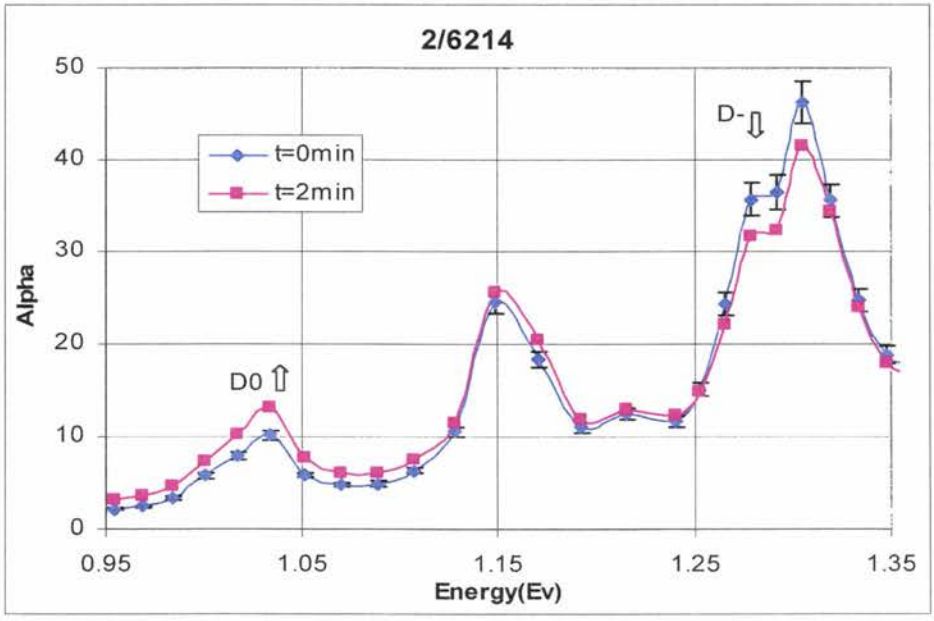

Figure 4.9: Sub-Gap absorption of 2/6214 around 1.1 eV and 1.3 eV .

Kinetics of the Trap Conversion Process:

A simple model for trap-to-dangling bond conversion has been developed by Dr. Dalal. The notations used in the model equations are explained below:

D_0 - be the density of neutral dangling bonds at time t = 0

D - be the density of neutral dangling bonds at any time t

N_0 - be the density of negatively charged dangling bonds D^- at time t = 0

N - be the density of negatively charged dangling bonds D^- at any time t

σ- - capture cross section of the D^- state.

σ - Capture cross section of the D state

n - Number of electrons

p - Number of holes

μ_n - mobility of the electrons

τ_n - the life time of the electrons

G - Generation rate of the incident photons

v - Thermal velocity of the electrons.

c - Trap to dangling bond conversion rate constant

The photoconductivity can then be written as

$$\sigma_{ph} = qG\mu_n\varsigma_n \tag{4.1}$$

It is known from SRH recombination statistics that

$$\varsigma_n = \frac{1}{vD\sigma} \tag{4.2}$$

Since the D^- states already have two electrons, they are not going to capture any more electrons but they are good trap centers for holes (the minority carrier in our samples). Upon the absorption of a hole, the rate at which the N states get converted into D states is given by

$$\frac{dN}{dT} = -\frac{dD}{dT} = -cpN \tag{4.3}$$

Also $$p = G\varsigma_p \tag{4.4}$$

and $$\varsigma_p = \frac{1}{v\sigma_p(D + aN)} \tag{4.5}$$

where a is ratio of capture cross-sections between N and D states and σ_p is the capture cross- section of holes by D_0 states.

Thus $$\frac{dN}{dT} = -\frac{cNG}{v\sigma_p(D + aN)} \tag{4.6}$$

The total number of neutral dangling bond states at any time t will be given by

$$D = D_0 + (N_0 - N) \tag{4.7}$$

so putting it back in the previous equation

$$\frac{dN}{dt} = \frac{-cNG}{[v\sigma_p\{D_0 + N_0 + (a-1)N\}]} \tag{4.8}$$

Using non-dimensional variables, $d = \frac{D_0}{N_0}$ *and* $n_t = \frac{N}{N_0}$

$$[(d+1)(\frac{1}{n_t})+(a-1)]\frac{dn_t}{dt}=-cG \tag{4.9}$$

The solution to the above equation is [46]

$$(d+1)\ln(n_t-1)+(a-1)(n_t-1)=-cGt \tag{4.10}$$

from the above equation [4.10], it is clear that the time required to create a certain n_t, starting with a N_0 (n_t =1), is inversely proportional to the generation rate G. If the neutral dangling bonds created by trap conversion dominate the dangling bonds created by bond breaking (which is definitely going to be the case in oxygen doped samples) at very early degradation times, then the decay in photo-conductivity should be controlled by how many N_t states have converted into D_0, i.e. by (n_t -1). Since for a given (n_t -1), the time required to cause this change is inversely proportional to intensity, therefore the time required to cause a given photoconductivity decay should be inversely proportional to intensity.

In the Figure [4.10], the experimental decay curves for the oxygen leak-doped sample for the two intensities 1.5 sun and 0.75 sun are plotted. Then the 0.75 sun data is re-plotted by invoking the reciprocity of time and intensity, and the result is shown in the Figure by symbol Δ. The time converted curve maps almost perfectly at early times (when few additional dangling bonds have been generated by the bond-breaking model) onto the experimental curve for 1 sun degradation thus proving the kinetic relationship postulated in Equation 4.10.

To verify that it is not an isolated case this plot was made for other samples which verified the results of the model. One another such plot for sample 2/6353 (with different O concentration) is shown in Figure [4.11].

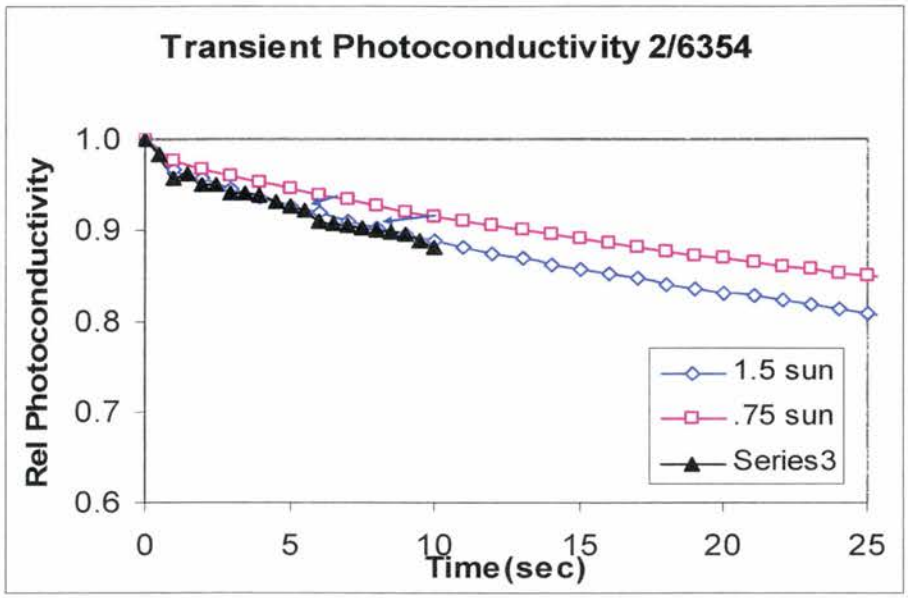

Figure 4.10: Transient decay showing the inverse relationship between the Intensity and time for a given degradation supporting equation 4.10.

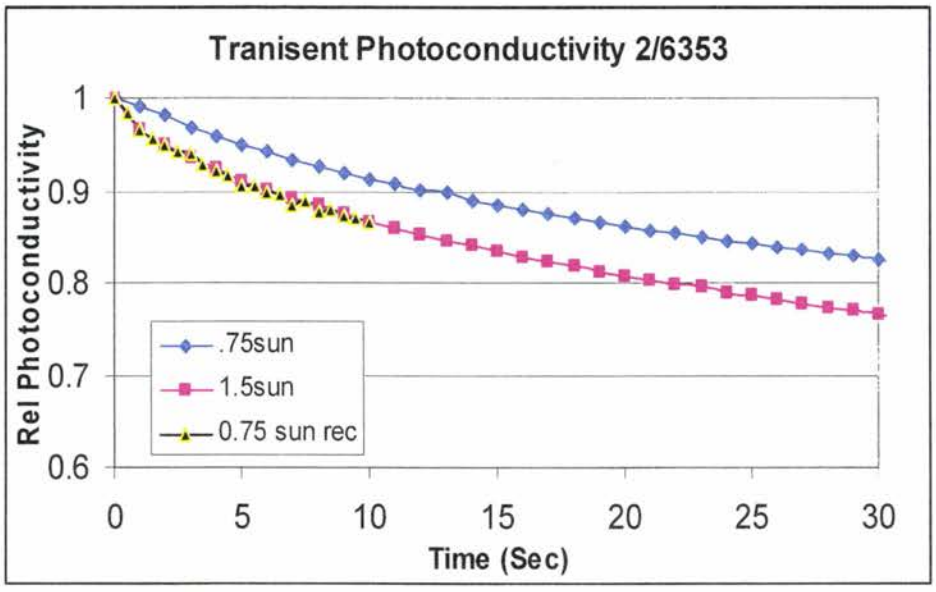

Figure 4.11: Transient decay showing the inverse relationship between the Intensity and time for 2/6353 another of O doped samples.

CHAPTER 5

CONCLUSIONS

The experimental data has clearly shown for the first time that the negatively correlated negatively charged states that exist in the gap convert into neutral dangling bonds during the initial stages of degradation of doped films. An analytical model has been verified to explain the conversion of charged dangling bonds into neutral bonds upon mono-molecular trapping, and the intensity behavior matches the model very well. An increase in the oxygen concentration, which creates more D- states, leads to a more pronounced decrease in absorption at ~1.3 eV, implying that the negatively charged, negatively correlated dangling bond at that energy have converted into a neutral dangling bond at ~1.1 eV below the conduction band. This result matches the prediction of Adler's model, and been proved for the first time. Since oxygen is common accidental donor in a-Si:H, it is not surprising that the previous work found a non-linear behavior between the mid-gap alpha and inverse of photoconductivity and since these studies were made for whole of the sub gap absorption, the said changes have been absorbed at a different energy level while other studies have been made at a particular energy level. Thus these series of results have proven the role of negatively charged states during the degradation of a-Si:H which has been doubted for a long time and these results should definitely help in the better understanding of the problem and the remedial steps that need to be taken to tackle this problem in future.

FUTURE WORK

The contamination of films with O has clearly shown the role of negatively charged defect states into increase of neutral dangling bonds during the light induced degradation. In the future, a systematic study can be done on these films while incorporating some donor states in the films and study their effects during early degradation times. These donor states can be attached by doping from group five elements in the periodic table like ppm levels of phosphine.

pip structures (which will have only one type of carriers) can be made and see if similar changes in sub-gap spectra occur upon hole injection.

REFERENCES

1. Staebler, D. L. and Wronski, C. R., Appl. Phys. Letters 31, 292 (1977)

2. Hirabayashi, I., Morigaki and Nitta, Jpn. J. Appl. Phys., 19 (7), L357 (1980)

3. Dersch, H., Stuke, J., and Beichler, Appl. Phys. Letters, 38 (6), 456 (1981)

4. N. B. Goodman, Philos. Mag. B 45, 407 (1982)

5. M. Grunewald, K. Weber and P. Thomas, J. Phys. (Paris) colloq. 42, C4-523 (1981)

6. D. V. Lang, J. D. Cohen, and A.M. Sergent, App. Phys. Letters 40, 474 (1982)

7. J. L. Pankove, J. E. Berkeyheiser, Appl. Phys. Letters 37, 705 (1980)

8. N. M. Amer, A. Skumanich and W. B. Jackson, Physica (Utrecht) 117 & 118B, 897 (1983)

9. J. Kakolios, R. Street, W Jackson, Phys. Rev. Lett. 59, 1037 (1988)

10. P. Stradins, H. Fritzsche, Philos. Mag B 69, 121 (1994)

11. Rana Biswas, B.C. Pan, Solar Energy Materials and Solar Cells (2002) in Press

12. Howard M. Branz, Phys. Rev. B , 59, 8 (1999)

13. Li You Yang and Liang Fan Chen, MRS Symp. Proc. 297, 619 (1993)

14. Stephan Heck and Howard M. Branz, MRS Symp. Proc. 664 A.12.2.1 (2001)

15. Paul Stradins, Satoshi Shimizu, Michio Kondo and Akihisa Matsuda, MRS Symp. Proc. 664 A12.1.1 (2001)

16. J. Pearce, G. Ganguly, R.W. Collins and C.R. Wronski, MRS Symp. Proc. 664 A.12.3.1 (2001)

17. D.E Carlson, C.R Wronski, App. Phys. Letters 28, 671 (1976)

18. S. Guha, J. Yang, A. Banerjee, IEEE Trans. On Electron Devices 46, 2080 (1999)

19. K. Tanaka, E. Maruyama, T. Shimada, "Amorphous Silicon" John Wiley, 1999

20. D. Redfield and R.H. Bube, Proc. IEEE Photovoltaic Sp. Conf., 1506 (1990)

21. D.E. Carlson, Properties of Amorphous Silicon and its alloys, T. Searle, EMIS Data Reviews Series No. 19, 264 (1998)

22. S. Guha, J. Yang, A. Banerjee, Proc. IEEE Photovoltaic Sp. Conf. 563 (1997)

23. D. Adler, Journal de Physique, 42, Suppl. C-4,1 (1981)

24. V.L. Dalal, B. Stafford, E. Sabisky, eds. New York: American Institute of Physics, 249 (1987)

25. Riemer, J.A., Vaughn, R.W and Knights, J.C, Physical Review Letters, vol 44, no3, p 193-196, Jan 1980

26. H. Branz and M. Silver, Phys. Rev. B 42, 7420 (1990)

27. M. Fathallah, Philos. Mag. B 61, 403 (1990)

28. K. Morigaki, I. Hirabayashi, and Nitta, Solid State Commun. 33, 851 (1980)

29. H. Fritzche, Solid State Commun. 94, 953 (1995)

30. V. L. Dalal, T. Maxson and Kay Han, J. Non-Cryst. Solids, 227, 1257 (1998)

31. S. Matsuo and M Kiuchi, Proc. Symp. VLSI Sci. Technol. Electrochemical Soc., Pennington, NJ, 83 (1983)

32. M. Pontoh, V.L. Dalal, Neha Gandhi, Proc. Of Matter. Res. Soc., 715, A 19.6 (2002)

33. J.R. Doyle, D. Doughty and A. Gallagher, J. Appl. Phys.,68,4375 (1990)

34. A. Matsuda and K. Tanaka, J. Non-Cryst. Solids, 97-98, 1367 (1987)

35. J Perrin, G. Brunno, P. Capezzuto and A. Madan, Academic, San Diego, 216 (1995)

36. V.L. Dalal, J. Non-Cryst. Solids, 395, 173 (2000)

37. Heavens, O.S, "Optical Properties of Thin Solid Films" New York Academic Press, 1955

38. Mott and Davis, "Electronic Processes in Non-Crystalline Materials", Oxford University Press, Oxford 1979

39. J. Tauc, "Optical Properties of Solids", North Holland, Amsterdam, (1970)

40. K. Seeger," Semiconductor Physics, an Introduction", Springer-Verlag, New York (1991)

41. Madan," Amorphous Silicon Semiconductors- pure and hydrogenated", Materials Research Society, c1987, Pittsburg, PA.

42. S. Lee, S. Kumar and C. Wronski, J. Non-Cryst., Solids, 114, 316 (1989)

43. Bullot, J., P. Cordier, M. Gauthier, Philos. Mag. B 61, 413 (1990)

44. Proefschrift ,"Growth Related Material Properties of Hydrogenated Amorphous Silicon" Eindhoven University of Technology, 2002, ISBN 90-386-1969-3

45. Simmons, J. G., Taylor, G. W., Phy. Review B 4, 502 (1971)

46. Dalal, V., Sharma, P., Ahmed Aziz," Evidence for Trap conversion instability in hydrogenated Amorphous Silicon" MRS Symp. Proceedings, to be published.

ACKNOWLEDGEMENTS

First and foremost, I would like to express my sincere gratitude to my major professor, Dr. Vikram Dalal, for his invaluable guidance and support through out my graduate studies. I would like to thank him for accepting me to do the research work in his group and for his sincerity towards his students. I would also like to thank Dr. Gary Tuttle and Dr. Rana Biswas for serving on my committee.

I would also like to thank Keqin Han, Jason Zhu, Matt Welsh who helped me with sample preparation and invaluable assistance and suggestions. Thanks also to Aziz Ahmed whose measurements at the start of research were also used for understanding the model.

I would also like to thank Max Naock for his technical help and healthy discussions we had during this time.

Also special thanks go to Jane Woline for helping me in all possible ways - cheering up and motivating to do well.

I would also like to thank my friends here at MRC -Matt Ring, Josh Graves, Durga Prasanna Panda, Kamal Muthukrishnan, Andy Niu, my roommates and friends who always gave me good support.

Finally I would like to thank my mother and father for their support, patience and love during my school years. They have always been a motivating force behind me to perform better. Thanks also to my brother Sumeet for supporting me in every possible way.